DOI
https://doi.org/10.18690/um.fkkt.1.2024.5

ISBN
978-961-286-829-1

Influence of Ammonium Polyphosphates and 2,4,6-Triamino-1,3,5-Triazine on the Mechanical-Physical Properties of Polyurethane and Alkali-Activated Materials

Branka Mušič, Barbara Horvat

Slovenian National Building and Civil Engineering Institute, Ljubljana, Slovenia
branka.music@zag.si, barbara.horvat@zag.si

In building constructions, the tendency towards an ever-better material directs us to composite materials. In this work, we prepared an organic-organic and organic-inorganic composite material by incorporating fire retardants, ammonium polyphosphates, and 2,4,6-triamino-1,3,5-triazine, into a polyurethane network and an aluminosilicate network (ASN) of alkali-activated material. Polyurethane foams (PUR) are well-known materials that, due to their properties, such as low weight-to-strength ratio, low electrical and thermal conductivity, flexibility, and relatively simple preparation process, are used in various industries, also in the construction industry, e.g., for thermal insulation of windows and doors or fixing and sealing joinery. Opposite, the ASN of alkali-activated metakaolin, successfully paves the way for new applications, such as high-temperature protection. In this paper, these interactive properties of prepared composites are studied using thermal testing and mechanical analysis. It was found that inhibitors significantly increase the fire resistance of PUR systems while they slightly reduce the mechanical properties. Incorporating polymer flame retardant into ASN in building products, such as façade panels, can decrease the mechanical properties but can offer the non-flammable building envelope not get heated from burning surroundings, i.e., not becoming a convection heat source, but rather represent a fire-distinguisher for flammable materials.

Keywords:
flame retardants,
polyurethane,
alkali-activated metakaolin,
microwave irradiation,
mechanical properties

University of Maribor Press

1 Introduction

Presently, organic halogenated compounds are industrially used fire retardants for various materials as they are required in low concentrations, typically 0.5–1 m% (HBCD use in EPS for Building Applications, ICL-IP Europe BV, 06/07/2014). However, halogenated fire retardants are phased out (HBCD banned since 20164b, currently used alternatives are also organic halides) due to their proven or suspected hazardous effects on the environment and health (Covaci et al., 2006). On the other hand, halogen-free fire retardants are more environmentally friendly with very low toxic potential and are not yet industrially viable. The most frequently studied halogen-free fire retardants are inorganic, IHF-FR (nano oxides, layered clays, hydroxides, etc.), phosphorus-containing compounds, and nitrogen-rich compounds. Those are used as synergistic agents to improve fire retardant properties as their dominant fire retardant mechanism is associated with the dilution of flammable gases, cooling the fire zone, the formation of an effective protective layer during combustion, or the presence of adsorption-desorption sites for combustion gases (Laoutid et al., 2009). Their inclusion in various construction products, such as polyurethane foams and alkali-activated materials, could provide many advantages, such as reducing stiffness and brittleness, improving the durability and longevity of the new composite material, while at the same time increasing the benefits for the users of the construction product, and due to environmental soundness, it allows manufacturers to recycle the material after its life more easily. This is especially beneficial in the building and construction industry to lower its negative environmental footprint, i.e., the building and construction industry annually consumes nearly 70 m% of Mount Everest's mass of raw materials and generates more than 30 m% of the world's waste (Miller et al., 2023 and Dyrud et al., 2023).

Polyurethane foams are materials known for a long time in the market. Their use has increased over the years due to their unique properties, such as low weight-to-strength ratio, low electrical and heat conductivity, better environmental and fire safety, flexibility in the method of application, quick and easy use due to the fast hardening reaction, and relatively easy process of preparation. Due to the listed properties, polyurethane foams are used in various industries, including construction, e.g., for thermal insulation of windows and doors or fixing and sealing joinery. They can even be used as an insulating material on walls and roofs. By

decreasing flammability, i.e., by incorporating halogen-free fire retardants ammonium polyphosphates and 2,4,6-Triamino-1,3,5-triazine, the environment and the fire safety of the whole community can become significantly more protected.

On the other hand, flame-retardant polymeric materials can be used as additives in alkali-activated materials which are not as well-known on the market as polyurethane foam. Alkali-activated materials are very thermally stable and non-flammable but to achieve better mechanical properties, such as reducing stiffness, polymer materials can be added to them, thus showing better properties/flexibility. The selected polymers for forming the composite with alkali-activated materials are flame-retardant polymers with the desire to have as little influence as possible on the inflammability of alkali-activated materials when included in the aluminosilicate network (ASN). Nevertheless, both the PUR and AAM composite systems can exhibit poorer compatibility with the selected polymers, which harms their dispersion in the matrix, which is why studies were made in this presented research work.

In the present research, we tested two completely different construction-industrial materials, polyurethane foam (PUR) and a non-combustible potential substitute for types of cement, mortars, and ceramics, i.e., alkali-activated material (AAM) based on metakaolin and Na-silicate solution where alkali-activated slurry was additionally cured in its early stage by microwaves at 100 W for 1 minute to increase the amount of the ASN. We studied the influence of the used halogen-free fire-retardant polymers – ammonium polyphosphates (APP) and 2,4,6-triamino-1,3,5-triazine (TATA) on the composite systems PUR-APP, PUR-TATA and AAM-APP, and AAM-TATA.

2 Methods – evaluation of the input material

To be able to evaluate the effect of the added flame retardants APP and TATA on all four composite systems PUR-APP, PUR-TATA and AAM-APP, and AAM-TATA separately, we had to study both the input raw materials and analyze the final composites in detail. Both flame retardant additives used were commercially available. First was ammonium polyphosphate, Exolite AP 422 (APP) supplied by Clariant (Mutenz, Switzerland). It is a white fine powder, non-hygroscopic, non-flammable, halogen-free, with a bulk density of 700 kg/m^3, and a melting point of

~240 °C. The second used fire retardant material was 2,4,6-Triamino-1,3,5-triazine (TATA) supplied by Sigma Aldrich (St. Louis, MO, USA). It is white powder, with a bulk density of 800 kg/m^3 and a melting point of ~354 °C. As the basic polyurethane foam for the preparation of new composite materials, we have chosen commercially available the two-component polyurethane foam "Tekapur Polefix" (PUR), supplied by TKK d.o.o. (Srpenica, Slovenia). The Tekapur Polefix contains component A, which is a polyol with several hydroxyl groups and triethyl phosphates, and component B, which is polymethylene polyphenyl polyisocyanate. Chemical evaluation of the metakaolin (MK), a precursor used to prepare the AAM material (noted as Mix 5, reference), and also the AAM composites (AAM-APP noted as Mix 6 and AAM-TATA noted as Mix 7) was performed by X-ray fluorescence using XRF (Thermo Scientific ARL Perform'X Sequential XRF) and by determining the amount of organic compound and carbonates, from the loss on ignition (LOI) for 2 hours at 550 °C and 950 °C, respectively. To determine the quantitative mineralogical composition of used MK, mineralogical analysis was carried out by Rietveld refinement, using corundum Al_2O_3 as an external standard, on X-ray powder diffraction (XRD, Empyrean PANalytical X-ray Diffractometer, Cu X-Ray source) patterns. The precursor was first dried, milled, and further sieved below 125 μm for LOI, XRF, and XRD. Results were reported in published scientific research (Horvat et al., 2023 and Horvat et al., 2022c), as well as the optimal mixture of MK and used alkali (Na-silicate solution, Geosil, 344/7, Woelner, Ludwigshafen, Germany, 16.9% Na_2O, 27.5% SiO_2). The theoretically determined mass ratio (using software in MS Excel platform developed in project No. C3330-17-529032 "Raziskovalci-2.0-ZAG-529032" and upgraded in the ARRS project under Grant No. J2-3035) between MK and liquid alkali was 1:0.66, respectively. For the synthesis, however, MK was used as it was received.

We performed some additional analysis on the incoming raw materials, as follows.

For both powder fire retardant input raw materials, scanning electron microscopy (SEM; Jeol JSM-IT500, low vacuum conditions) was performed at 500-x magnification (BED-S, Sta.-PC 60 and 20 kV). The differences in size and shape are shown in Figure 1.

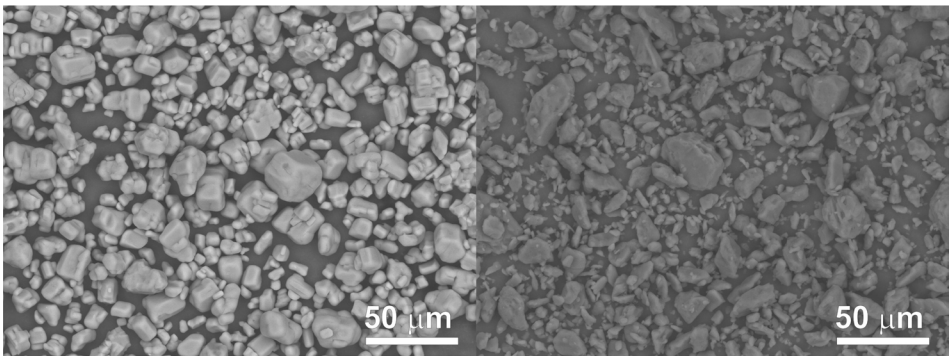

Figure 1: SEM analysis of fire retardants APP (left) and TATA (right).
Source: own.

APP powder is slightly larger than TATA powder, has more rounded edges, and is more regular in shape while TATA has a very wide distribution of irregularly shaped particles.

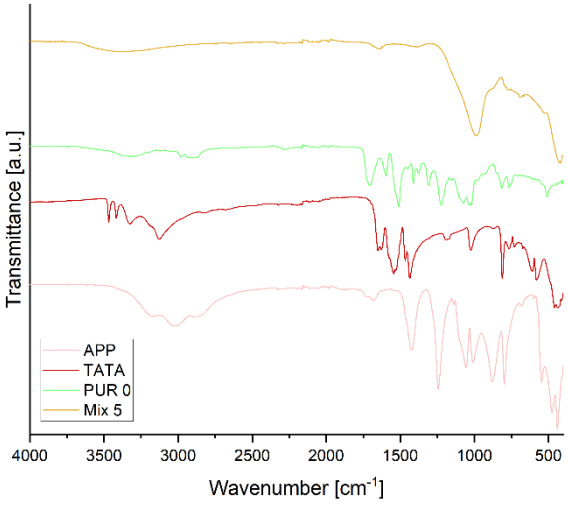

Figure 2: FTIR spectrum of input materials.
Source: own.

Additionally, FTIR and XRD analysis for all input materials that compose the final PUR and AAM composites were evaluated. Those input materials were APP, TATA, Mix 5 (AAM without additives, reference), and pure PUR (noted as PUR 0,

reference). FTIR was performed by Fourier transform infrared spectroscopy (FTIR; PerkinElmer Spectrum Two, ATR mode) – it is represented in Figure 2. XRD was performed by X-ray powder diffraction (XRD; Empyrean PANalytical X-ray Diffractometer, Cu X-Ray source) – it is represented in Figure 3.

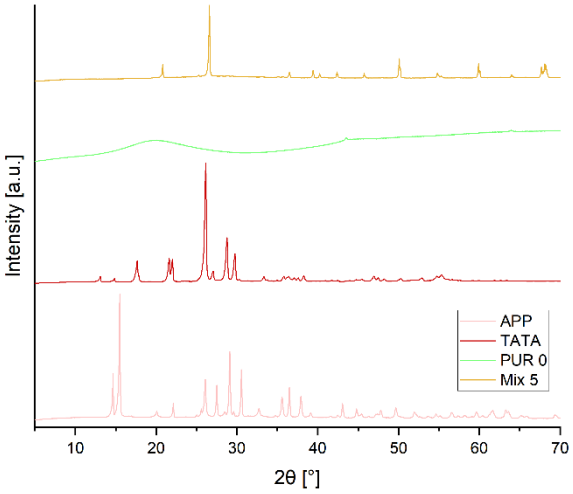

Figure 3: XRD pattern of powder raw materials.
Source: own.

Both analyses were later used to determine the effect of the addition of selected fire retardant additives on the prepared final PUR and AAM composites.

3 Methods – preparation of the composite material

Due to the completely different nature of AAM and PUR materials, which were used as base, support materials for preparing our new composites, we also had to incorporate the fire-resistant polymer materials, APP and TATA, respectively, in a slightly different procedure.

Preparation of PUR samples: The appropriate amount of PUR component B (polyisocyanate) and a flame retardant, APP or TATA, were weighted into a mixing vessel and mixed with a high-speed mechanical stirrer at about 1400 rpm for 10 min to obtain a homogeneous mixture (PUR 0 was without flame retardants and served as reference). After that, the appropriate amount of component A (polyol) was

poured into the mixture which was further homogenized with a stirrer at 1000 rpm and transferred into a mold with enough free space to enable the full expansion of the foam during curing. The foams were stored for 72 hours at room conditions T = 23 °C ± 2 °C (noted as T0) and relative humidity 50% ± 15% in accordance with ISO 291:2008. The structure and resulting performance of polyurethane foams are driven by the stoichiometry of the polymerization reaction which is directly impacted by applied monomers, additives, their chemical composition, and the ratio between the polyols and isocyanates (Hejna et al., 2017, Amran e tal., 2021, Fink e tal., 2018). The ratio used in PUR 0 between polyol and isocyanate was according to the manufacturer's recommendations. Therefore, the mixing weight ratio was 1:1.22. The reference PUR foam (PUR 0) with the addition of APP was designated as PUR 1 and the foam with the addition of TATA was designated as PUR 2. From preliminary research, we found that a maximum of 30% of the fire-retardant additive can be included in the system based on the total weight of the A + B component so that the fire-retardant powder is homogeneously mixed into the B component. In Table 1 the masses of the used ingredients for PUR samples are given.

Table 1: Masses of the used ingredients for PUR samples.

Specimens	Comp. A (g)	Comp. B (g)	APP (g)	TATA (g)
PUR 0	32.7	40.0	0.0	0.0
PUR 1	32.7	40.0	21.8	0.0
PUR 2	32.7	40.0	0.0	21.8

Preparation of AAM samples: MK with added defined amounts of APP and TATA, respectively, was previously homogenized with a laboratory vibrating ball mill (MixMill MM20, Danfoss, Slovenia). The mechanical grinding process (homogenization) took place at room temperature for 3 minutes at a frequency of 30 Hz. 3 hardened stainless steel balls with a diameter of 0.8 mm were used in a 50 mm^3 stainless steel drum. Then, the powdered raw materials (finely homogenized MK with the addition of APP and finely homogenized MK with the addition of TATA) were mixed with a Na-silicate solution and water, as shown in Table 2, until the material was completely wet at 1000 rpm. The amount of added water was determined experimentally to reach sufficient wetting of all solid powders in the mixture.

Table 2: Masses of the used ingredients.

Mixture	MK [g]	Alkali [g]	APP [g]	TATA [g]	H_2O [g]
Mix 5	74.9	33.0	0.0	0.0	7.5
Mix 6	50.0	33.0	24.9	0.0	30.0
Mix 7	50.0	33.0	0.0	24.9	7.5

The mixtures were put into molds made of silicone-urethane rubber. The presented mixtures in Table 2 were evaluated after the curing procedure, which was irradiating fresh slurry with microwaves (frequency 2.45 GHz, inverter microwave, Panasonic, NN-CD575M) for 1 min at 100 W (positively influencing the dissolution of reagents while dehydration is not yet severely affected (Horvat et al., 2022b) and additionally further curing at room conditions for 14 days).

Geometrical densities along with mechanical bending and compressive strengths were measured after 14 days of curing of AAMs in the conditioning room. For the evaluation of mechanical strengths, the compressive and bending strength testing machine (ToniTechnik ToniNORM) was used.

4 Results – composite materials

As mentioned in the "preparation of the composite material" section, AAM and PUR materials are very different. In Figure 4 and Figure 5 below, therefore, we present a visual representation of our test samples. Observing the pictures, we can get a sense of the visual appearance and internal texture of the samples.

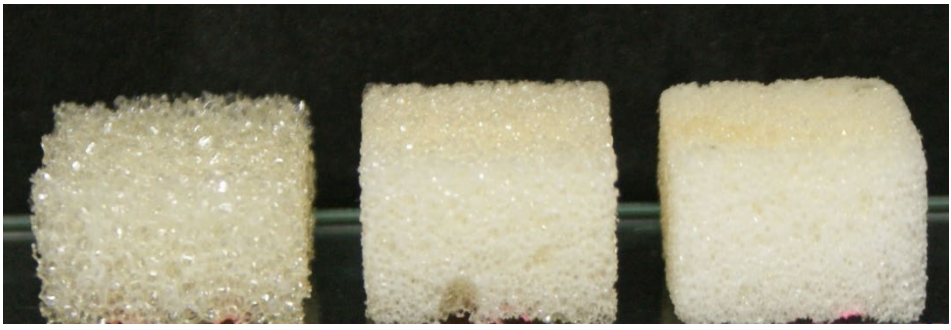

Figure 4: Prepared PUR samples from left to right: PUR 0, PUR 1, and PUR 2.
Source: own.

Figure 5: Images of sample Mix 5, sample Mix 6, and sample Mix 7 (from left to right).
Source: own.

Figure 5 shows how much APP affects the structure formation of the Mix 6 sample.

To show the visual difference between our test samples in even more detail, we also made the SEM analysis of prepared and hardened mixtures of both PUR (Figure 6) and AAM composites (Figure 7). The PUR images were taken at magnification 40x (BED, NOR, Std. PC 60 and 20 kV).

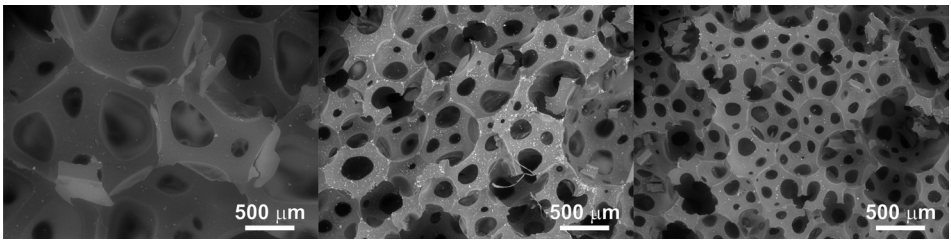

Figure 6:. SEM images of prepared, hardened samples (from left to right) PUR 0, PUR 1, and PUR 2.
Source: own.

It can be seen in the pictures, that both flame retardant additives affect the formation of the skeletal network of polyurethane foam as the pore sizes of PUR 1 and PUR 2 significantly decreased.

In Figure 7, SEM images of AAM composites are presented with a scale of 100 µm, recorded at 150x magnification (BED, NOR, Std. PC 60, and 20 kV). The marked places in Figure 7 show the cracks in the material.

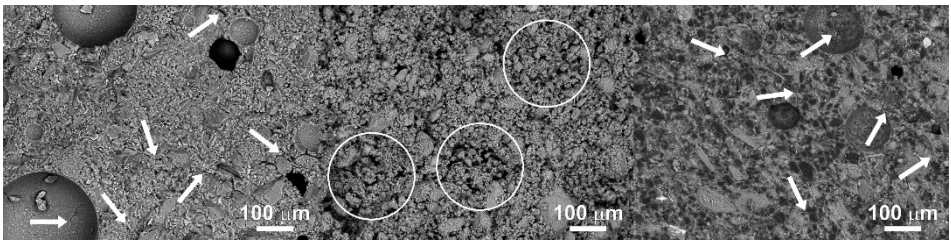

Figure 7: SEM images of prepared, hardened samples (from left to right) Mix 5, Mix 6, and Mix 7.

Source: own.

In all three cases, cracks appeared in the hardened samples Mix 5, Mix 6, and Mix 7, with the largest visible in Mix 6 and the smallest in Mix 7. In Mix 5, cracks are due to dehydration while bubbles are due to the mixing of ingredients (there was no gas formation in the chemical reaction of alkali and MK) where some air bubbles got permanently caught. The highly porous structure in Mix 6 is due to the reaction of APP with alkali, which leads to the release of health-harmful gasses and prolongation of curing. The least porous material, according to SEM, is Mix 7 where TATA was added. TATA did not react with alkali but just filled the empty spaces in the ASN network where it got well encapsulated and stored for the case of fire.

AAM materials are known as very good temperature-resistant materials. Therefore, we tested their response to elevated temperatures. Each sample was cured at room temperature (T0) and then treated at several temperatures at 250 °C, 500 °C, 750 °C, and 1000 °C (laboratory oven Memmert for temperature 250 °C and for higher temperatures furnace Protherm). After the temperature treatment, mechanical strength was evaluated. The remaining broken pieces show the response to temperature. They are shown in Figure 8.

The thermal behaviour of polyurethane foam is also important because the PUR foams are insulators. Therefore, their thermal insulation and flammability are important. In Figure 9, you can see the response to fire of PUR 0, PUR 1, and PUR 2 according to the UL-94 HB standard.

In Figure 9, we can see that in PUR 0, the line is no longer visible after 30 seconds of burning while in the case of PUR 1 with the fire-retardant additive APP and in

the case of PUR 2 with the flame-retardant TATA, the line was still visible after 30 seconds of burning. TATA in PUR 2 works even better because, in the case of PUR 1 with APP additive, we see that the sample started to sag.

Figure 8: From top to bottom, samples of Mix 5, Mix 6, and Mix 7 are shown in temperature treatments from left to right: T0, 250 °C, 500 °C, 750 °C, and 1000 °C.

Source: own.

The thermal conductivity of the PUR specimens was determined in a homemade heat flow setup. The dimensions of the specimens were (100 mm x 60 mm x 10 mm) x 1 mm. Thermal conductivity was determined on the specimens inserted in between cold and hot plates with temperatures of 15 °C and 25 °C, respectively. The thermal conductivity of the specimens are as follows PUR 0 (36.5 mW/mK), PUR 1 (36.4 mW/mK), PUR 2 (35.6 mW/mK). Presented values correspond well to the

apparent densities of the specimens as a higher density (also visible from SEM images of PUR 1 and 2 composites) of the cellular insulation generally contributes to increasing its thermal conductivity. The apparent densities of the PUR specimens were determined according to ISO 845:2006. The densities of the PURs are as follows: PUR 0 (46.70 kg/m^3), PUR 1 (62.61 kg/m^3), and PUR 2 (60.04 kg/m^3). The densities of PUR 1 and PUR 2 are comparable and about 30% higher than PUR 0 (Mušič et al., 2022).

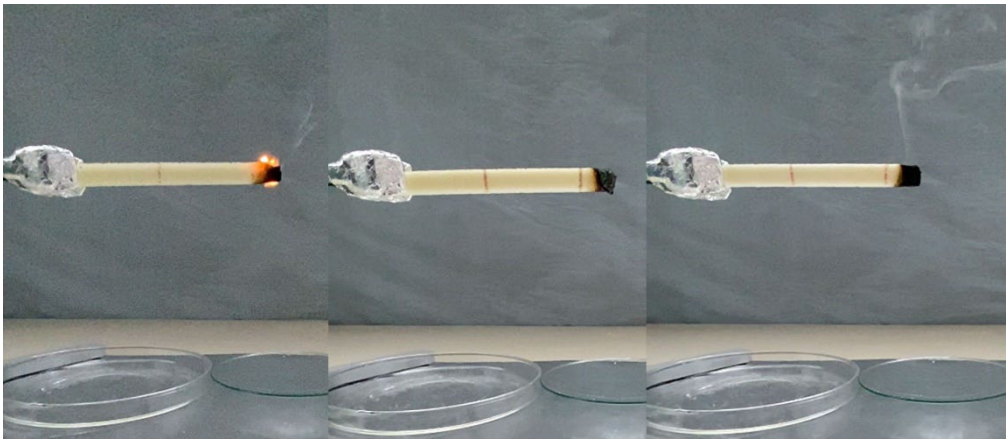

Figure 9: A Horizontal burning test of PUR 0, PUR 1, and PUR 2 samples (from left to right), after 30 s of burning.
Source: own.

The interesting behaviour of AAM composites with increasing temperature was also observed through the distribution of pore sizes and the change in skeletal density.

The pore distribution and skeletal density of the AAM materials were measured by mercury intrusion porosimetry (Micromeritics autopore IV, mercury porosimeter, Series 9500). The pore distribution of heat-treated AAM samples is shown in Figures 10 – 12.

In Figure 10, it can be seen that the size of the distribution of pores moves towards higher values. The changes at about 250 °C are attributed to the dehydration of the material (water leaves the material and on this account the pores increase). As

expected, the bigger differences in the "size of the pores" occurred at 1000 °C which we attribute to the larger cracks that appeared in the material (see Figure 8).

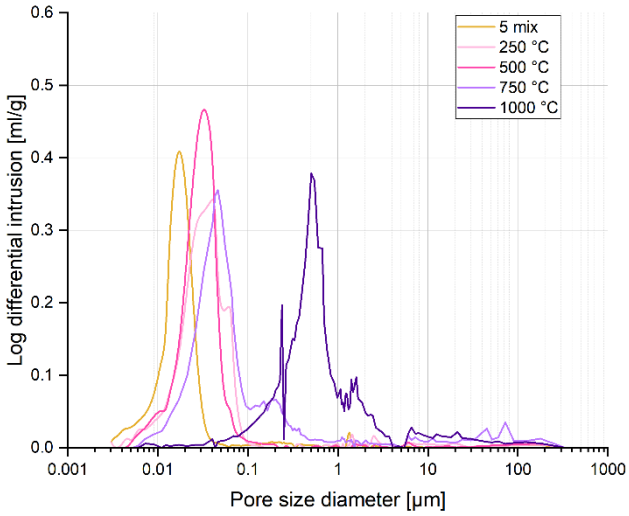

Figure 10: Pore size distribution of Mix 5 samples at different temperature treatments.
Source: own.

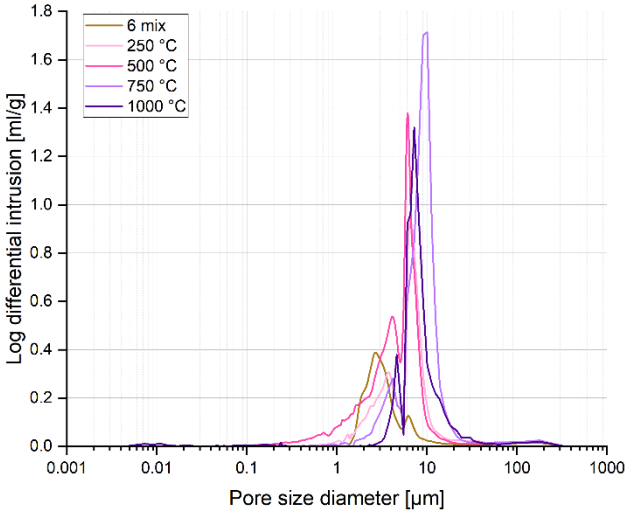

Figure 11: Pore size distribution of Mix 6 sample at different temperature treatments.
Source: own.

In Figure 11, we can see that the original sample Mix 6 at T0 is much more porous than the sample Mix 5. Therefore, it is possible to observe here that with increasing temperature, there is a significantly smaller shift of the peaks to the right towards larger values of the pore size distribution than at sample Mix 5. In Figure 8, we can see that in the case of Mix 6, there were much greater visual differences after temperature treatment, which was also reflected in the mechanical properties presented in the rest of the article.

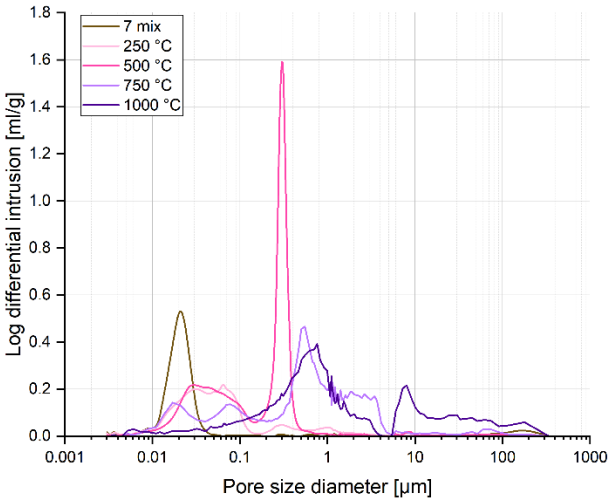

Figure 12: Pore size distribution of Mix 7 sample at different temperature treatments.
Source: own.

Figure 12 shows that at lower temperatures, the pores are smaller and the material is more stable. At around 250 °C, the effect of dehydration of the material is known and the pores partially increase while at ca. 500 °C, the process of thermal decomposition begins and complete decomposition of TATA occurs at slightly more than 700 °C which is also expressed in the increase in the distribution of pores.

It can be seen from Figures 10-12 that the smallest pores in the AAM composite material are formed by Mix 5 while the largest is by Mix 6.

We also observed the behaviour of PUR composites after the addition of fire retardant additives, as we changed the pore size distribution (Figure 13), total porosity (Figure 14), and skeleton density (Figure 15) with it.

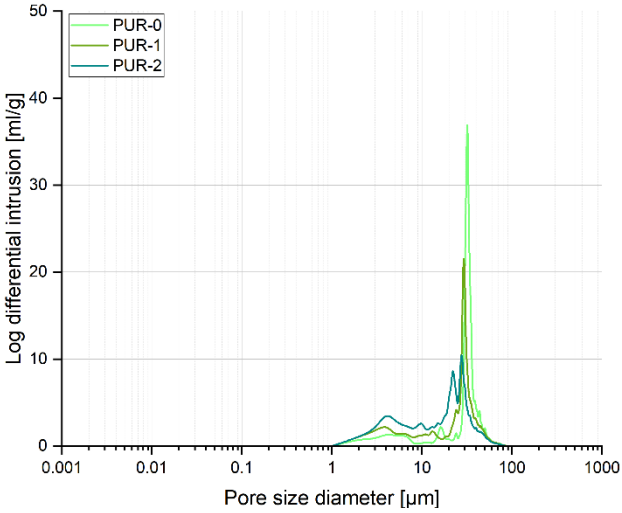

Figure 13: Pore size distribution of PURs at different fire retardant additives.
Source: own.

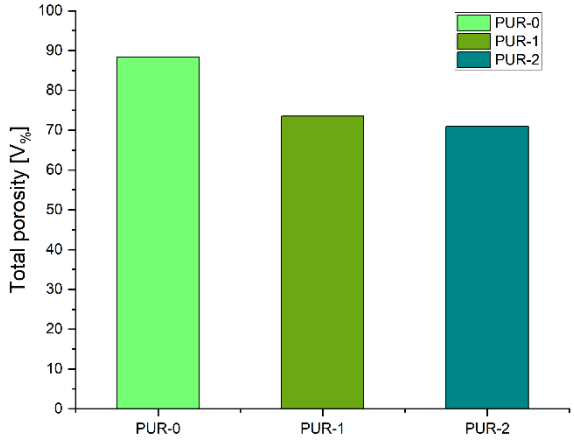

Figure 14: Total porosity of PURs at different fire retardant additives.
Source: own.

It is expected that in PUR 1 and PUR 2 the total porosity decreases, as the fire retardants fill the empty pore spaces, which are the largest in PUR 0.

This also changes the skeletal density, which we measured both for PURs composites (Figure 15) and for AAM composites (Figure 16).

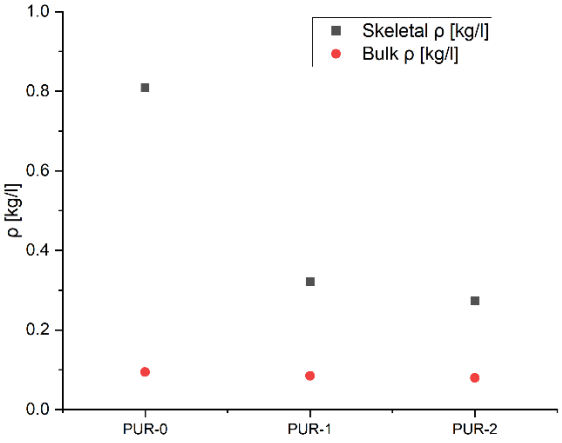

Figure 15: Skeletal and bulk density of PURs at different fire retardant additives.
Source: own.

In Figure 15, we can see that while the bulk density remains the same, the skeletal density changes strongly with fire retardant additives.

It can also be seen that the increasing temperature impacts the densification of the material skeleton. The skeletal density is shown below in Figure 16.

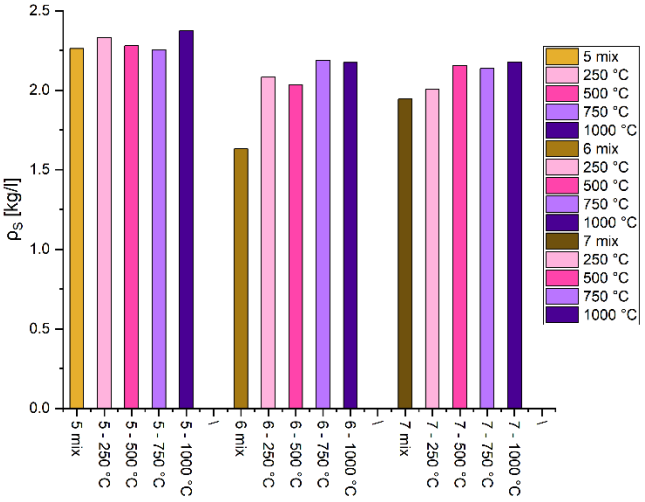

Figure 16: Skeletal density of Mix 5, Mix 6, and Mix 7 at different temperature treatments.
Source: own.

As expected, Mix 5 exhibits the highest skeletal densities (Mix 5 is without organic compounds) while the skeletal densities of Mix 6 and Mix 7 samples are comparable and lower.

However, observing the measurements shown, we have seen that the addition of flame retardant materials affects the physical and mechanical properties of the composites. So, we additionally measured the bending and compressive strength.

The compression and bending behaviour of the PUR specimens were determined on a universal test machine Zwick Z030, Zwick Roell Group, Ulm, Germany. Compression properties were determined according to EN 826:2013. The test specimens were compressed between the two plates of the universal test machine. At a constant rate of 0.5 mm/min, they were applied to the specimen till failure occurred. Bending behaviour was determined according to the requirements of EN12089:2013. The specimens were tested in three-point bending mode in a universal test machine. At a constant rate of 0.5 mm/min, failure occurred. The compressive and bending properties of the specimens are summarized and presented in Table 3. The (σ_M (MPa) represents compressive strength and σ_b (MPa) bending strength.

Table 3: Mechanical properties of PURs.

Specimens	σ_M (MPa)	σ_b (MPa)
PUR 0	335 ± 19	293 ± 6
PUR 1	220 ± 11	260 ± 9
PUR 2	314 ± 16	253 ± 19

The compression and bending strength of the AAM samples were determined on a laboratory test machine (and were measured with ToniPRAX (ToniTechnik, Berlin, Germany) at a force rate of 0.05 kN/s). The compressive and bending properties of the AAM samples are presented in Figures 17 and 18.

Strengths were also measured on PUR samples. We measured using a Durometer device, according to EN ISO 868:2004. Durometer hardness is a dimensionless quantity. It represents a relative comparison of hardness between different but similar classes of materials where hardness is measured at the same durometer scale. A Shore A hardness tester (Zwick, Ulm, Germany) was used.

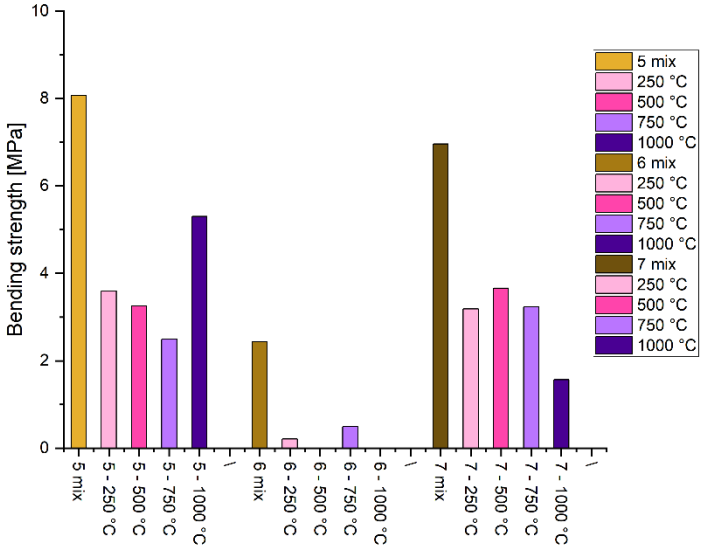

Figure 17. Bending strength of samples Mix 5, Mix 6, and Mix 7 at different temperature treatments.

Source: own.

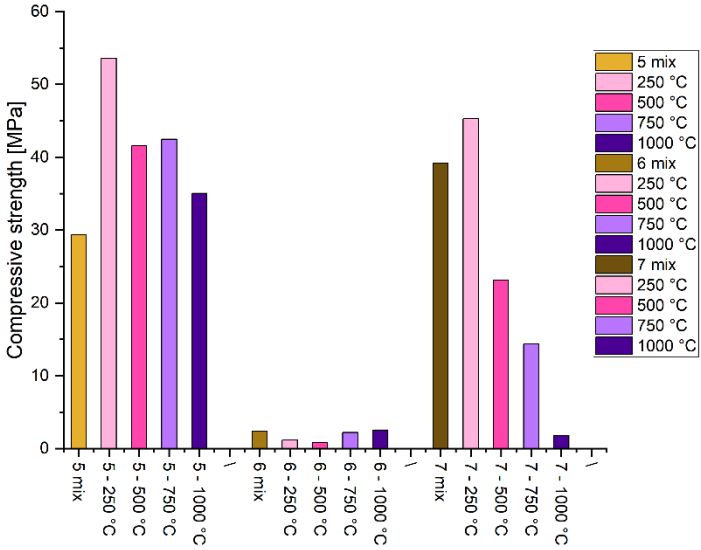

Figure 18. Compressive strength of samples Mix 5, Mix 6, and Mix 7 at different temperature treatments.

Source: own.

Shore hardness measurements also showed differences between the samples with the pristine pure PUR 0 sample once again having higher hardness (Shore A Durometer Hardnesses around 30) than PUR 1 (Shore A Durometer Hardnesses around 16) and PUR 2 (Shore A Durometer Hardnesses around 16 Hardnesses around 14) where an organic flame retardant additive was added.

The changes due to the added APP and TATA which were manifested in the different formation of the network structure in PUR 0, PUR 1, and PUR 2 (which we saw in Figure 1 and the different pore sizes in Figure 2) also impact the hardness of the materials due to polymer additives. Of course, the influence of APP and TATA on the flammability of PUR materials was also expressed in the XRD analysis. Below, Figure 19 shows the XRD pattern of all three PURs, the original PUR 0, PUR 1, and PUR 2.

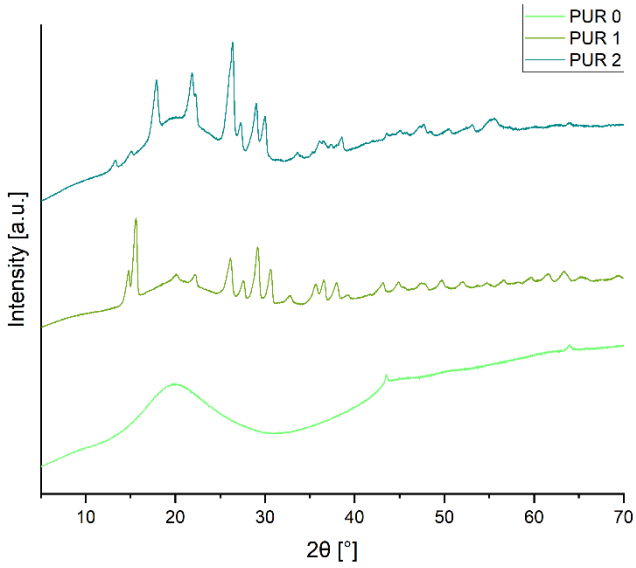

Figure 19: XRD patterns of PUR samples.
Source: own.

Also, the chemical influence of APP and TATA addition on AAM is evident from the FTIR spectrum (Figure 20).

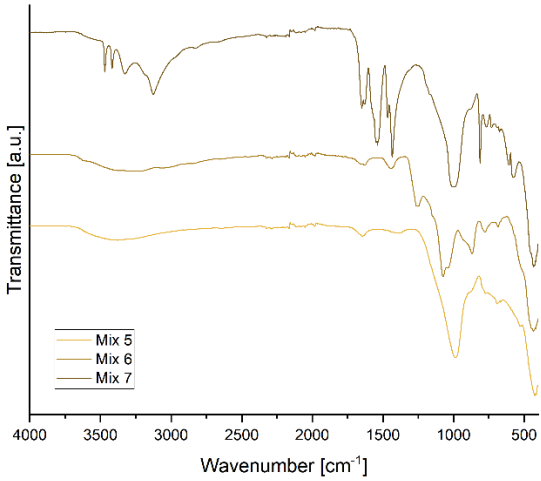

Figure 20: FTIR spectrum of the AAM materials Mix 5, Mix 6, and Mix 7.
Source: own.

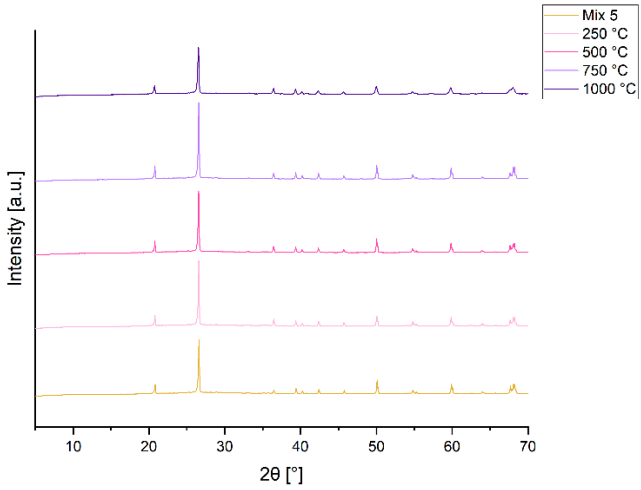

Figure 21: XRD pattern of the sample Mix 5 at different temperature treatments.
Source: own.

If we compare the FTIR spectrum of the powdered raw materials in Figure 2 and the FTIR spectrum of the AAM composite materials in Figure 20, we can see that there is no induced chemical reaction at room temperature in cases of Mix 5 and Mix 7 while in the case of Mix 6, we can see that the change is occurred (even during the mixing of the APP with alkali the gases released).

The XRD pattern presented in Figure 21-23 shows that with increasing temperature in samples Mix 6 and Mix 7, there were changes in curves while in Mix 5 there were no changes.

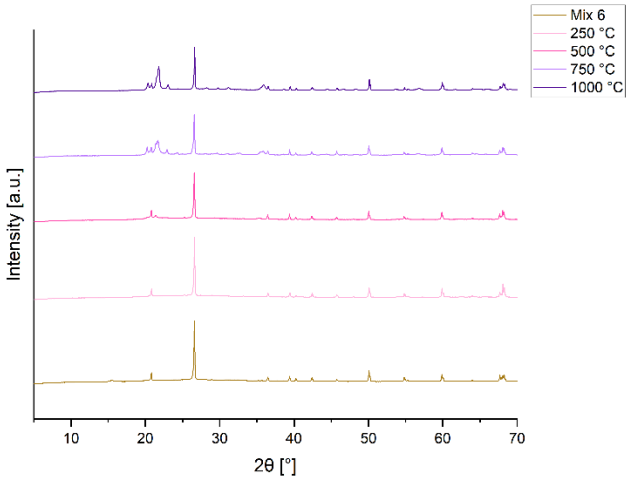

Figure 22: XRD pattern of the sample Mix 6 at different temperature treatments.
Source: own.

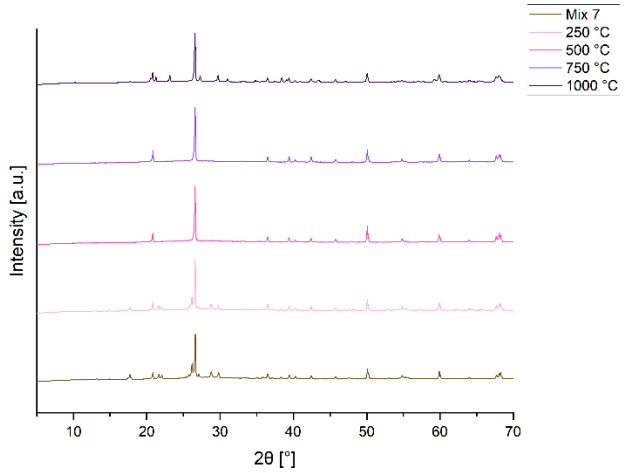

Figure 23. XRD pattern of the sample Mix 7 at different temperature treatments.
Source: own.

In Figure 21, the XRD pattern of Mix 5, it is seen that there are no changes up to 1000 °C and the material is very temperature stable. In Figure 22, the XRD pattern of Mix 6, it is seen that at temperatures T0 and 250 °C, we cannot see the presence of APP which was dissolved in an alkali solution. At 500 °C, we can see the beginning of the mineralogical changes in sample Mix6 which are even more visible at temperatures 750 °C and higher. In Figure 23, the XRD pattern of Mix 7, the presence of TATA is seen up to 500 °C. We can also see the appearance of new compounds at 750 °C and 1000 °C (similar to the pores size distribution behaviour).

5 Conclusions

In the present work, two polymer additives that are used as flame retardants are included in two completely different materials by chemistry, final properties, and the purpose of use. In PURs, which are used as insulating materials, fire-retardant properties were increased while in AAM materials which are non-flammable, fire-retardant material that does not react with alkali got well encapsulated in the ASN where it is permanently stored for the case of the fire in the surrounding materials.

Flame retardants reduced the strength and stress in the PUR polymer matrix. Additives APP and TATA still maintained satisfactory mechanical properties of PURs although the hardness of PUR 1 and PUR 2 weakened and both, TATA and APP, significantly reduced inflammation.

The mechanical properties of AAM composites with APP and TATA are inferior compared to pure AAM, especially for APP. The combinations of fire retardant powders and AAM reduce the density. Flame retardants have expectedly better and greater positive effects on PUR than AAM.

Acknowledgment

This work is part of the ARRS project of Barbara Horvat, Ph.D., and was financially supported by the Slovenian Research Agency under Grant No. J2-3035 and also by Slovenian Research Agency program group no. P2-0273.

References

Amran U.A., Salleh K.M., Zakaria S., Roslan R, Chia C.H., Jaafar S.N.S, Sajab M.S, Mostapha M., 2021, Production of Rigid Polyurethane Foams Using Polyol from Liquefied Oil Palm Biomass: Variation of Isocyanate Indexes. Polymers, 13, 3072.

Covaci A., Gerecke A.C., Law R.J., Voorspoels S., Kohler M., Heeb N.V., Leslie H., Allchin C.R., De Boer J., 2006, Hexabromocyclododecanes (HBCDs) in the environment and humans: a review. Environ Sci Technol, 40(12):3679-88. doi: 10.1021/es0602492.

Dyrud A.M., Polluting the Pristine: Using Mount Everest to Teach Environmental Ethics, < https://peer.asee.org/polluting-the-pristine-using-mount-everest-to-teach-environmental-ethics> accessed 14 September 2023.

EN 826:2013. Thermal insulating products for building applications – Determination of compression behaviour.

EN 12089:2013. Thermal insulating products for building applications - Determination of bending behaviour.

EVS-EN ISO 868:2004. Plastics and ebonite – Determination of indentation hardness by means of a durometer (Shore hardness).

Fink, J.K.,2018, Poly(Urethane)s. In Reactive Polymers: Fundamentals and Applications; Elsevier, pp. 71–138, Amsterdam, The Netherlands

HBCD use in EPS for Building Applications, ICL-IP Europe BV, 06/07/2014, https://www.psloop.eu/wp-content/uploads/2023/08/Guide-for-PS-Loop_collection-and-pretreatment-of-EPS-waste_english.pdf accessed 31 Maj 2023.

Horvat B., Mušič B., Pavlin M., Ducman V., 2023. Microwave Irradiation of Alkali-activated Metakaolin Slurry, in: 5th International Conference on Technologies & Business Models for Circular Economy: Conference Proceedings. Presented at the International Conference on Technologies & Business Models for Circular Economy, University of Maribor Press, pp. 9–24. https://doi.org/10.18690/um.fkkt.1.2023.2

Horvat B., Pavlin M., Ducman V., 2022c. Influence of microwaves in the early stage of alkali activation on the mechanical strength of alkali-activated materials. Ceramics International. https://doi.org/10.1016/j.ceramint.2022.12.133.

Horvat B., Mušič B., Pavlin M., Ducman V., 2022b. Microwave irradiation of alkali-activated metakaolin slurry. Presented at the 5th International Conference on Technologies & Business Models for Circular Economy. https://doi.org/10.18690/um.fkkt.6.2022.

Hejna A., Haponiuk J., Piszczyk Ł., Klein M., Formela K., 2017, Performance Properties of Rigid Polyurethane-Polyisocyanurate/Brewers' Spent Grain Foamed Composites as Function of Isocyanate Index. Polymers, 17, 427–437.

ISO 291:2008 Plastics — Standard atmospheres for conditioning and testing.

ISO 845:2006. Cellular plastics and rubbers - Determination of apparent density.

Laoutid F., Bonnaud L., Alexandre M., Lopez-Cuesta J-M., Dubois P., New prospects in flame retardant polymer materials: from fundamentals to nanocomposites, 2009, Mat. Sci. Eng. R, 63, 100-125., https://doi.org/10.1016/j.mser.2008.09.002.

Miller, N.,. 2023, The industry creating a third of the world's waste <https://www.bbc.com/future/article/20211215-the-buildings-made-from-rubbish> accessed 25.August 2023.

Mušič B., Knez N., Bernard J., 2022, Flame Retardant Behaviour and Physical-Mechanical Properties of Polymer Synergistic Systems in Rigid Polyurethane Foams. Polymers, 14, 4616. https://doi.org/10.3390/polym14214616.

Shaw S.D., Blum A., Weber R., Kannan K., Rich D., Lucas D., Koshland C.P., Dobraca D., Hanson S, Birnbaum L.S., 2010, Halogenated flame retardants: do the fire safety benefits justify the risks? Rev. Environ. Health 25, 261–305.